

## STUDY OF SEISMIC BEHAVIOR OF INTERNAL REINFORCED CONCRETE BEAM-COLUMN JOINTS

Ahmed M Ismail<sup>\*1</sup>, Manar Abdel Shakour<sup>\*2</sup>, Ehab lofty<sup>\*3</sup>, Ibrahim Elkersh<sup>\*4</sup>

<sup>\*1,2,3,4</sup>Faculty of Engineering Suez Canal University, Egypt

### ABSTRACT

Beam-Column joints are crucial structural elements in a seismic force resisting system. Failure of these elements may lead to total collapse of a structure. Recent earthquakes have demonstrated that structural systems designed based on current codes of practice are vulnerable to severe damages, mostly due to undesirable performance of joints. In general, design codes do not consider the effects of joint characteristics on the behavior of the structure and treat joints as members which remain elastic during an earthquake. To thoroughly understand the effects of different design parameters on the behavior of beam-column connections in reinforced concrete (RC) structures and consequently on the overall performance of seismic force resisting system, a wide range of experiments must be carried out. But prior to a successful setup and conducting any experiments, a theoretical study and numerical simulation is essential. Therefore, it is necessary to study the behavior of RC beam-column joints subjected to seismic forces using a F.E. model for RC beam-column connections in the simulation environment provided by ANSYS, and then investigate the performance of beam-column joint.

In the first part of this research, a verification study using ANSYS 21 for 9 full-scale reinforced concrete with the presence additional reinforcement at the joint core and debonding of reinforcement in some joints. The verification study aims to compare the experimental results with numerical results. It can be concluded that the finite element analysis was performed numerically, and the predicted seismic performance was in very good agreement with the experimental results. The second part of this research is the numerical modeling of twenty four beam column joint specimens were modeled using the ANSYS 21 program. The modeling was similar for all beam column joints specimens.

Several wide beam specimens were simulated in this research to reveal the stress transfer paths in wide beam-column joints. Models with greater (significantly more than 1.0) shear capacity ratios, VR, and moment capacity ratios, MR, have the capabilities to resist forces with magnitudes 70% up to 100% more than code requirements. More specimens should be considered to improve the understanding of load paths of wide beam-column connections with various geometries and design parameters, such as beam width and depth, column height, beam-to-column eccentricity.

### 1. INTRODUCTION

Earthquakes are a destructive natural hazard that directly or indirectly impact human civilisation, or even the geology at locations adjacent to the epicentre of earthquakes. Numerous recorded disasters have happened in different places around the world as a consequence of earthquakes. Many buildings have been damaged, or even destroyed due to ground shaking, causing numerous human casualties and great economic impacts. Typical examples include the 1992 Cairo earthquake in Egypt. Buildings were damaged or destroyed in these events due to either the direct ground motion or indirect events that happened after the main quake, such as tsunami or nuclear accidents. In order to protect people and their property, buildings and infrastructure should be able to withstand the main earthquake, aftershocks and the following events. However, it is nearly impossible to mitigate or prevent the impacts resulting from the indirect effects of earthquakes since such activities are complicated and unpredictable. Therefore, the most important and practical thing is to ensure that buildings and constructions remain safe under direct ground shaking.

In the past, reinforced concrete structures were designed without any consideration for seismic-resistant design philosophy. Nowadays, people are becoming more and more aware of the consequences of these disastrous events to society and the economy, and different design methods have been employed to avoid, or at least mitigate the adverse effects due to earthquakes. Traditionally, only the performance of buildings and the seismic hazards in high seismicity regions were investigated since people usually thought that buildings in moderate and low seismicity regions were fine. Later on, it was found that even in moderate seismicity regions, severe damage on buildings could still happen and so codes of practices were extended to take account of the effects due to moderate seismic excitations.

Occurrences of recent earthquakes in different parts of the world and the resulting losses, especially human lives, have highlighted the structural inadequacy of buildings to carry seismic loads. The great losses due to the Cairo earthquake on October 1992 (Ms 5.4) were mainly related to the fact that at the time of construction, the buildings

were designed to resist only vertical loads and had insufficient lateral resistance. Thus, the columns and beam-column connections were found to have inadequate shear capacity, ductility, and confinement in plastic hinges.

So there is an urgent need for assessment of existing buildings in terms of seismic performance and to continuously upgrade the seismic codes for the design of new buildings. The design of structures for earthquakes became a major demand enforced in the Egyptian design codes [1] that motivated the Ministry of Housing and Buildings to update the Egyptian codes regularly, taking into account the seismic loads. Since October 1992, a set of Egyptian codes have been released to prevent building collapse and/or control major damages of structural elements. Many advances in earthquake engineering have been made from the observation of the performance of real structures that have been subject to a severe earthquake. Analytical modeling, including finite element analysis, has an important role, but its limitations must be recognized. For many engineered structures, satisfactory seismic performance requires careful attention to analysis, design, and detailing and good construction practice. Safety is thus achieved by the successful integration of analysis, design, and construction.

## 2. VERIFICATION MODELS

The numerical simulation becomes a primary factor in a huge number of scientific papers. In structural field, researches have used the numerical models as an acceptable way for simulating almost all structural elements to figure out the main factors that affect their performance and to improve characteristics of these elements using specific additions or different unique reinforcement details. These models have quietly replaced the tradition build and break models. The present research is basically based on numerical analysis for studying the behavior of RC beam-column joints subjected to seismic forces. The numerical used models in this research are conducted by the well-known finite element software (ANSYS 2021 R2). ANSYS is a large scale multipurpose program that is used in almost all engineering disciplines: aerospace, automotive, electronics, manufacturing, energy services, nuclear, plastics, and steel industries.

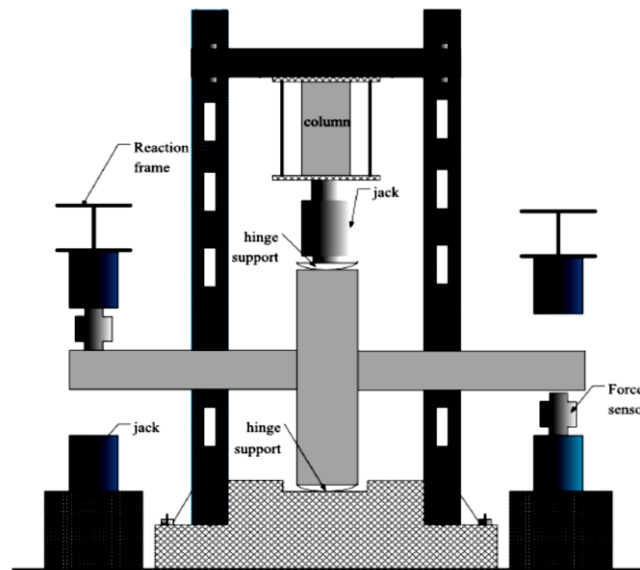


Fig1: Test Setup

In this research, a verification of JianBing Yua experimental work [2] is conducted. The experimental program of this research was designed to investigate the seismic behavior of 9 full-scale reinforced concrete (RC) joints—8 precast RC joints and 1 cast-in-place RC joint—under cyclic loading. The precast concrete (PC) joints were divided into 3 types: cast-in-place, precast beam cast-in-place column, and fully precast with assembly. With the presence additional reinforcement at the joint core and debonding of reinforcement in some joints, the PC joints differed with other types of joints. The experimental results, such as hysteretic behavior, energy dissipation capacity and stiffness degradation, were analyzed, which showed that the PC joints with steel strands anchored into the joint core zone could meet the seismic code requirements. Additionally, a finite element analysis of the new type of PC joint was performed numerically, and the predicted seismic performance was in very good agreement with the experimental tests.

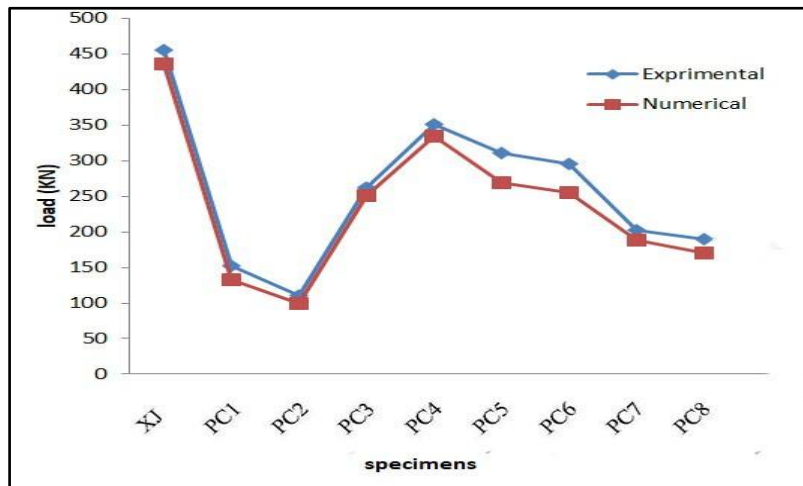


Fig2: Comparison between numerical and experimental failure load results

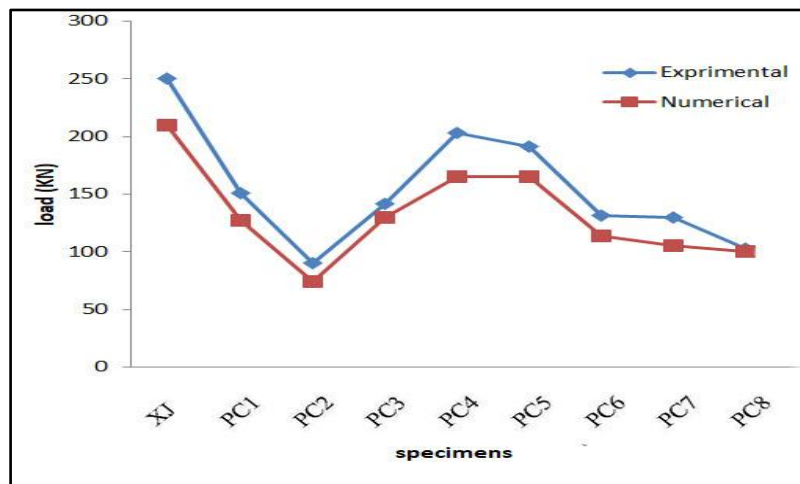


Fig3: comparison between numerical and experimental first crack results

### 3. NUMERICAL STUDY

#### Virtual Test (Simulation) Setup:

To Develop a F.E. model for RC beam-column connections in the simulation environment provided by ANSYS 21, in order to study the behavior of RC beam-column joints subjected to seismic forces using the developed model, main goal of this research is to investigate the performance of the RC beam-column under cyclic and pushover tests, including displacement ductility and ultimate strength.

Test specimens were divided to six groups with different parameters under study. The numerical program aimed to investigate effect of parameters on ultimate strength, displacement and ductility behavior. All considered joints are designed to comply with the specifications of ACI design manual for high seismic regions [3].

#### a) Parametric study:

Effect of loading type, effect of column moment of inertia, effect of beam moment of inertia, effect joint transverse steel ratio and effect of ties reinforcement ratio.

#### b) Finite element modeling

Three element types are used in the ANSYS program, namely; SOLID65 for concrete and adhesive epoxy, LINK180 for steel reinforcement, and SOLID185 for steel plates and supports.

#### c) Model generation

From six series of models (which are developed based on two classes of models defined in Table 1 and four different joint transverse steel ratios, 24 different F.E. models called B11 through C34 with specified configurations provided in Tables 1 and 2 were generated.

Table (1) Column dimensions and reinforcements for two classes of models

Class of Model	Column Cross Section (mm <sup>2</sup> )	Column Steel Ratio	Beam Tension Steel ratio	Ties	Stirrups
B	300×300	0.04	0.012	Φ14 @80mm	Φ10 @80mm
C	300×450	0.04	0.012	2Φ12 @80mm	Φ10 @80mm

Table (2) Joint reinforcement for different models

Model Series	Beam Cross Section (mm <sup>2</sup> )	Joint Transverse Steel Ratio			
		Type1	Type2	Type3	Type4
B1	300×300	0.017	0	0.005	0.030
B2	300×450	0.017	0	0.005	0.030
B3	300×600	0.017	0	0.005	0.030
C1	450×300	0.006	0	0.005	0.015
C2	450×450	0.006	0	0.005	0.015
C3	450×600	0.006	0	0.005	0.015

All the beam column joints specimens were modeled using the ANSYS program. The modeling was similar for all beam column joints specimens, shown below as an example. The beam column joint specimen model is defined as below:

The cross-section of the column was designed as 550 mm × 550 mm in dimension. Twelve 25 mm diameter bars (12B25) were adopted as the longitudinal reinforcements in the column, and 10 mm diameter bars were used as the stirrups with an interval of 100 mm (A10@100). The cross-sectional size of the beam was 300 mm × 550 mm, and the longitudinal reinforcements at the top and bottom of the beam were three 22-mm diameter bars (3B22) and three 18-mm diameter bars (3B18), respectively. Additionally, the middle of the beam contained two 10-mm diameters (2B10) steel bars. The stirrup interval was set to 100 mm in a 400 mm range from the left side to the right side in the joint. For the rest of the part, the stirrup interval was set to 200 mm.

The support plates is 100 x100 x10 mm while the loading plate is 200 x100 x10 mm as shown in Figure . The bond between steel reinforcement and concrete was assumed as perfect in the modeling of RC control beam specimen. The material properties are: concrete compressive strength,  $f_{cu} = 39.6$  MPa, steel yield 500 MPa.

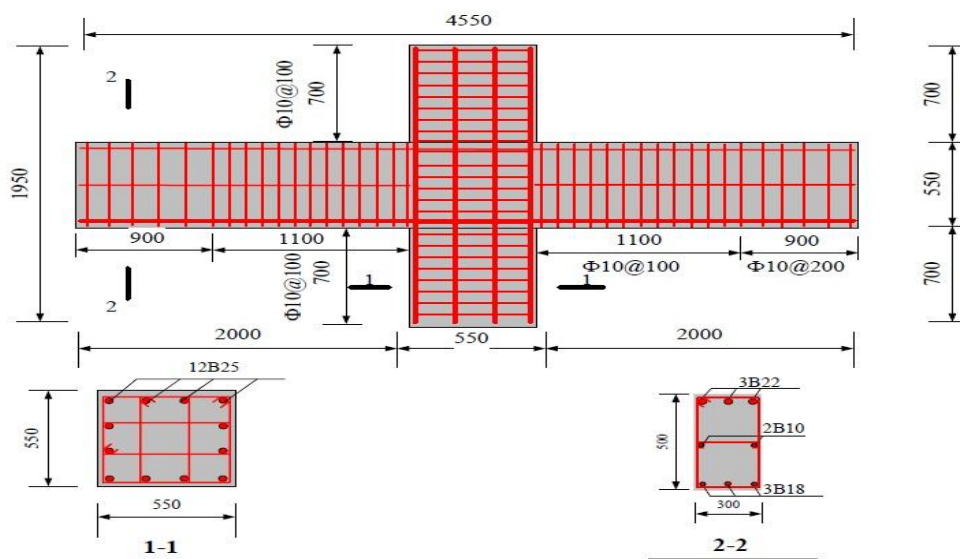


**Fig4: Internal reinforced concrete beam-column joint details**

**Table (3)** shows names of twenty four beam column joints and their description.

S.N	Model	Column Cross Section (mm <sup>2</sup> )	Beam Cross Section (mm <sup>2</sup> )	Column Steel Ratio	Beam Tension Steel ratio	Ties	Stirrups	Joint Transverse Steel Ratio
1	B11	300×300	300×300	0.04	0.012	Φ14 @80mm	Φ10 @80mm	0.017
2	B12	300×300	300×300	0.04	0.012	Φ14 @80mm	Φ10 @80mm	0
3	B13	300×300	300×300	0.04	0.012	Φ14 @80mm	Φ10 @80mm	0.005
4	B14	300×300	300×300	0.04	0.012	Φ14 @80mm	Φ10 @80mm	0.030
5	B21	300×300	300×450	0.04	0.012	Φ14 @80mm	Φ10 @80mm	0.017
6	B22	300×300	300×450	0.04	0.012	Φ14 @80mm	Φ10 @80mm	0
7	B23	300×300	300×450	0.04	0.012	Φ14 @80mm	Φ10 @80mm	0.005
8	B24	300×300	300×450	0.04	0.012	Φ14 @80mm	Φ10 @80mm	0.030
9	B31	300×300	300×600	0.04	0.012	Φ14 @80mm	Φ10 @80mm	0.017
10	B32	300×300	300×600	0.04	0.012	Φ14 @80mm	Φ10 @80mm	0
11	B33	300×300	300×600	0.04	0.012	Φ14 @80mm	Φ10 @80mm	0.005
12	B34	300×300	300×600	0.04	0.012	Φ14 @80mm	Φ10 @80mm	0.030
13	C11	300×450	450×300	0.04	0.012	2 Φ12 @80mm	Φ10 @80mm	0.006
14	C12	300×450	450×300	0.04	0.012	2 Φ12 @80mm	Φ10 @80mm	0
15	C13	300×450	450×300	0.04	0.012	2 Φ12 @80mm	Φ10 @80mm	0.005
16	C14	300×450	450×300	0.04	0.012	2 Φ12 @80mm	Φ10 @80mm	0.015
17	C21	300×450	450×450	0.04	0.012	2 Φ12 @80mm	Φ10 @80mm	0.006
18	C22	300×450	450×450	0.04	0.012	2 Φ12 @80mm	Φ10 @80mm	0
19	C23	300×450	450×450	0.04	0.012	2 Φ12 @80mm	Φ10 @80mm	0.005
20	C24	300×450	450×450	0.04	0.012	2 Φ12 @80mm	Φ10 @80mm	0.015

21	C31	300×450	450×600	0.04	0.012	2 Φ12 @80mm	Φ10 @80mm	0.006
22	C32	300×450	450×600	0.04	0.012	2 Φ12 @80mm	Φ10 @80mm	0
23	C33	300×450	450×600	0.04	0.012	2 Φ12 @80mm	Φ10 @80mm	0.005
24	C34	300×450	450×600	0.04	0.012	2 Φ12 @80mm	Φ10 @80mm	0.015

**d) Support conditions**

For all models, support conditions are defined to be capable of simulating lateral loading for real seismic loads. As shown in Fig. 12b joint supports are pinned on three sides and fixed on the fourth side.

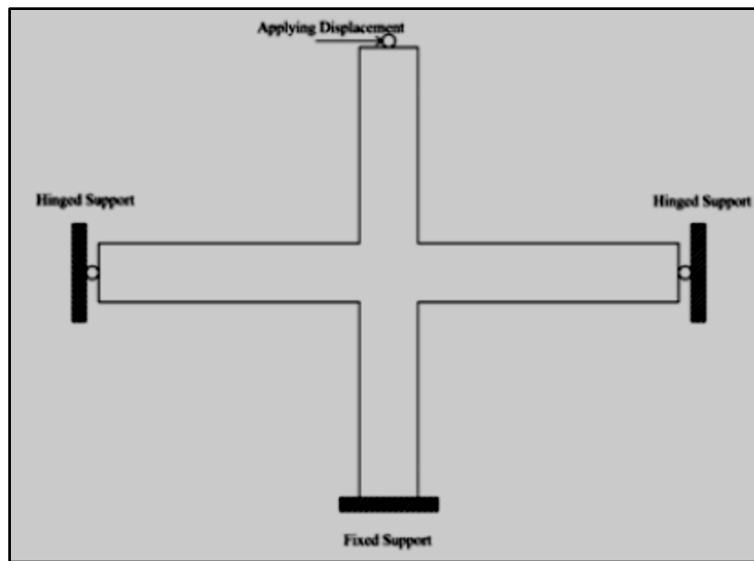


**Fig5: Supports conditions**

**e) Loading**

Two different loading patterns are applied to the simulated models. Both patterns are displacement control type. The first pattern is pushover loading type where displacement increases up to failure of connection. The second pattern is cyclic loading in which displacement increases in two different directions at the magnitude of 0.02 meters per each step and remains the same for three cycles per each step. Except for the first two steps where displacement increases by 0.01 meters per step.

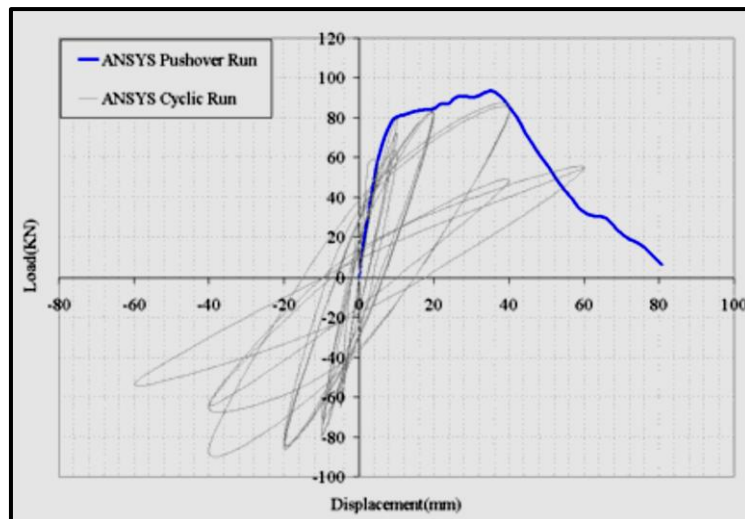


**Fig6: Comparing Pushover and Cyclic curves for the model**

#### f) Analysis

Two different types of analysis, which depend on loading patterns, are used to analyze the models. Type one is used for pushover analysis and presents results of pushing the structure in several steps, from beginning to failure. In type two a transient dynamic load with push and pull cycles is applied as cyclic loading. Results are presented at three points in each cycle, maximum point, minimum point and onset point (where displacement is zero).

#### e) Meshing

Mesh generation is one of the influential steps that affects the accuracy and precision of results. For regular prismatic bodies, eight-node cube solid elements are suitable to model a joint structure. Generally, for this type of element, accuracy depends on the size of the elements. By a lengthy process for finding a relatively efficient mesh size to get the best precision with minimum computational time, we found that a 50 mm cubic element is a suitable choice.

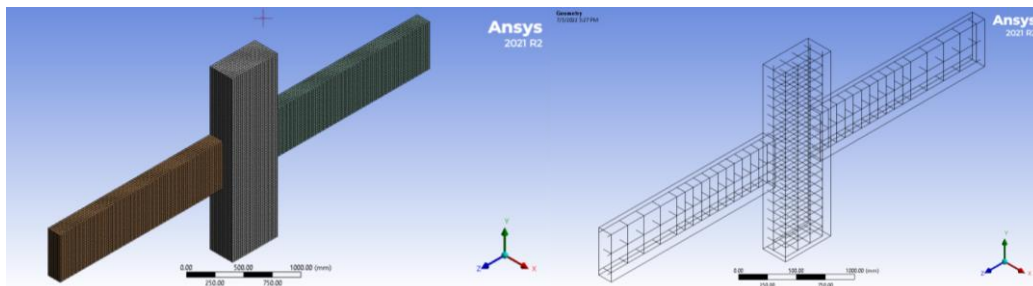


Fig7: Mesh of the concrete & reinforcement

#### Virtual Test (Simulation) Results:

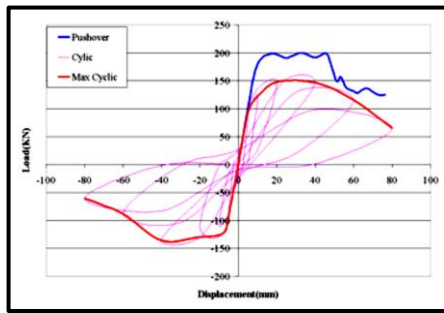
In this part shows results for twenty four beam column joints by using ANSYS. Displaying ultimate strength, displacement and ductility behavior for all beam column joints. All joints have different parameters such as column cross section, beam cross section, joint transverse steel ratio and type of ties. Out of all analysis outputs available in literature, we chose few appropriate results so as to be able to investigate the importance and performance of the following concepts: (i) load-displacement curves for pushover and cyclic loadings, (ii) drawing over-strength curves and (iii) determining displacement ductility,  $\mu$ , for joints. In the following section these concepts will be discussed in more detail.

#### Loading effect

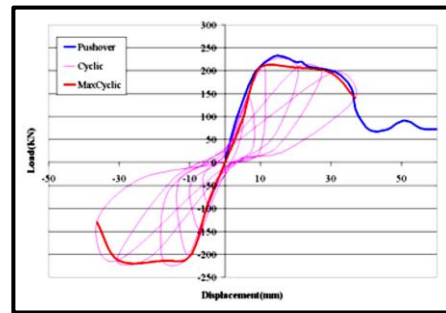
The performance of a joint and mainly its ultimate strength and displacement ductility under cyclic and pushover tests are compared and discrepancies are verified. Both pushover and cyclic load displacement curves are shown on the same graph. These graphs for some models are shown in Fig. 14. Backbone curves for cyclic-hysteretic loops are compared with pushover curves. By studying results for all models it can be seen that for most models, the hysteretic-loop-backbone curves move closely to pushover curves except for B1i and C1i models ( $i=1, \dots, 4$ ) which are one third of all considered models. For the remaining two thirds of models the difference is relatively small with an average of 6.58% (minimum of zero and maximum of 14%). It is almost a common error in most laboratory tests.

But for models B1i and C1i the average and maximum amounts of error are 25.1% and 32%, respectively. Such an error is not acceptable, but it might be justified by the beam heights for models B1i and C1i which are smaller than the heights of the beams in other models. So, in push and pull cycles crack propagation will increase faster than the other models. This conclusion can be raised from the fact that the reinforced confined core is placed in the middle of a beam and does not provide enough strength to prevent crack propagation.

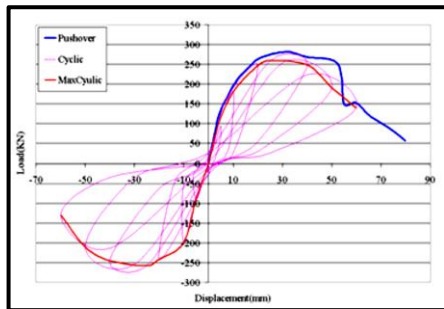
Next, we study the displacement ductility,  $\mu$ , which is defined as the ratio of the ultimate displacement of the model,  $\delta_u$  (where load decreases more than 15%), to yielding displacement,  $\delta_y$  (which is defined by equalized perfect elastic-plastic curve). To determine displacement ductility, the displacement from equating pushover and backbone curves must be equated to displacement from elastic perfect plastic diagrams. The displacement ductility of all models are determined and given in Tables 4 and 5.



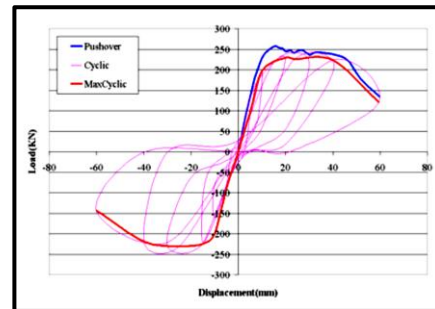
(a) Model B11



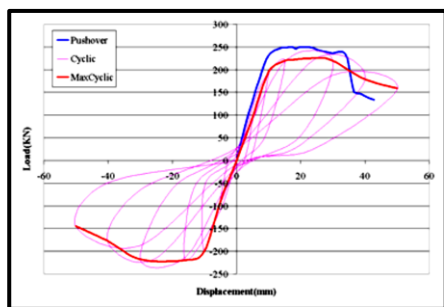
(b) Model B22



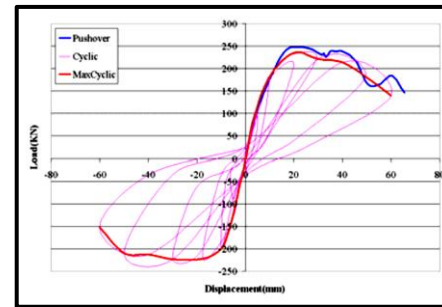
(c) Model B23



(d) Model C21



(e) Model C22



(f) Model C23

**Fig8: Comparing load-displacement curves from Pushover and Cyclic analysis**

Table (4) shows the ultimate strength, displacement and ductility behavior for all beam column joints under Cyclic loading:

S.N	Model	$\rho_s$	Moment capacity ratio MR	Yield disp. (mm)	Ult. disp. (mm)	$\mu$	(V ult)col (kN)
1	B11	0.017	3.80	17.5	55.0	3.1	146
2	B12	0.000	3.80	17.4	40.0	2.3	151
3	B13	0.005	3.80	17.6	48.0	2.7	148
4	B14	0.030	3.80	18.2	60.0	3.3	148
5	B21	0.017	1.87	18.0	56.0	3.1	231
6	B22	0.000	1.87	14.1	38.0	2.7	225
7	B23	0.005	1.87	18.0	46.0	2.6	231
8	B24	0.030	1.87	18.0	56.0	3.1	236
9	B31	0.017	1.08	15.0	26.0	1.7	240
10	B32	0.000	1.08	16.7	26.0	1.6	231
11	B33	0.005	1.08	16.0	26.0	1.6	240

12	B34	0.030	1.08	14.0	28.0	2.0	233
13	C11	0.006	3.80	20.0	47.2	2.4	165
14	C12	0.000	3.80	17.6	37.0	2.1	163
15	C13	0.005	3.80	18.6	44.0	2.4	165
16	C14	0.015	3.80	17.3	44.0	2.5	165
17	C21	0.006	1.88	21.3	48.0	2.3	258
18	C22	0.000	1.88	15.6	32.0	2.1	211
19	C23	0.005	1.88	19.6	44.0	2.2	234
20	C24	0.015	1.88	20.4	52.0	2.5	258
21	C31	0.006	1.08	13.8	29.0	2.1	214
22	C32	0.000	1.08	12.0	21.0	1.8	202
23	C33	0.005	1.08	14.0	27.0	1.9	220
24	C34	0.015	1.08	14.0	26.0	1.9	214

**Table (5) shows the ultimate strength, displacement and ductility behavior for all beam column joints under Pushover loading**

S.N	Model	$\rho_s$	Moment capacity ratio MR	Yield disp. (mm)	Ult. disp. (mm)	$\mu$	(V ult)col (kN)
1	B11	0.017	3.80	17.5	49.0	2.8	201
2	B12	0.000	3.80	17.4	33.0	1.9	193
3	B13	0.005	3.80	17.6	44.0	2.5	202
4	B14	0.030	3.80	18.2	51.0	2.8	218
5	B21	0.017	1.87	18.0	56.0	3.1	252
6	B22	0.000	1.87	14.1	34.0	2.4	251
7	B23	0.005	1.87	15.5	45.0	2.9	257
8	B24	0.03	1.87	15.7	55.0	3.5	272
9	B31	0.017	1.08	15.0	26.0	1.7	251
10	B32	0.000	1.08	16.7	20.0	1.2	251
11	B33	0.005	1.08	14.0	22.4	1.6	258
12	B34	0.030	1.08	14.0	25.2	1.8	274
13	C11	0.006	3.80	20.0	41.0	2.1	214
14	C12	0.000	3.80	17.6	30.0	1.7	211
15	C13	0.005	3.80	18.6	36.3	1.9	214
16	C14	0.015	3.80	17.3	45.0	2.2	221
17	C21	0.006	1.88	21.3	51.0	2.4	283
18	C22	0.000	1.88	15.6	31.3	2.0	231
19	C23	0.005	1.88	19.6	45.0	2.3	248
20	C24	0.015	1.88	20.4	49.0	2.4	292
21	C31	0.006	1.08	13.8	25.0	1.8	221

<b>22</b>	<b>C32</b>	0.000	1.08	10.0	15.0	1.5	211
<b>23</b>	<b>C33</b>	0.005	1.08	10.0	18.0	1.8	224
<b>24</b>	<b>C34</b>	0.015	1.08	14.0	26.6	1.9	230

**Table (6) Comparing ultimate loads results for model B1i and C1i (i=1, ..., 4)**

S.N	Models	Vult Push. (kN)	Vult Cycli (kN)	Difference (kN)	Difference Percentage %
1	B11	200	147.4	52.6	0.26
2	B12	192	149.0	542.5	0.22
3	B13	201	149.0	52.0	0.26
4	B14	219	149.0	70.0	0.32
5	C11	213	164.3	48.7	0.23
6	C12	212	162.0	50.0	0.24
7	C13	215	164.0	51.0	0.24
8	C14	220	166.5	53.5	0.24

**Table (7) Comparing displacement results for model B1i and C1i (i=1, ..., 4)**

S.N	Models	Δ ult Push. (kN)	Δ ult Cycli (kN)	Difference (kN)	Difference Percentage %
1	B11	49.0	55.0	-6.0	-0.12
2	B12	33.0	40.0	-7.0	-0.21
3	B13	44.0	48.0	-4.0	-0.09
4	B14	51.0	60.0	-9.0	-0.18
5	C11	41.0	47.2	-6.2	-0.15
6	C12	30.0	37.0	-7.0	-0.23
7	C13	36.3	44.0	-7.7	-0.21
8	C14	45.0	44.0	1.0	0.02

**Table (8) Comparing ultimate loads results for model B2i and C2i (i=1, ..., 4)**

S.N	Models	Vult Push. (kN)	Vult Cycli (kN)	Difference (kN)	Difference Percentage %
1	B21	253	230.0	23.0	0.09
2	B22	250	226.0	24.0	0.10
3	B23	258	230.0	28.0	0.11
4	B24	273	235.0	38.0	0.14
5	C21	282	259.0	23.0	0.08
6	C22	230	210.0	20.0	0.09
7	C23	249	235.0	14.0	0.06
8	C24	293	259.0	34.0	0.12

**Table (9) Comparing displacement results for model B2i and C2i (i=1, ..., 4)**

S.N	Models	$\Delta$ ult Push. (kN)	$\Delta$ ult Cycli (kN)	Difference (kN)	Difference Percentage %
1	B21	56.0	56.0	0.0	0.00
2	B22	34.0	38.0	-4.0	-0.12
3	B23	45.0	46.0	-1.0	-0.02
4	B24	55.0	56.0	-1.0	-0.02
5	C21	51.0	48.0	3.0	0.06
6	C22	31.3	32.0	-0.8	-0.02
7	C23	45.0	44.0	1.0	0.02
8	C24	49.0	52.0	-3.0	-0.06

**Table (10) Comparing ultimate loads results for model B3i and C3i (i=1, ..., 4)**

S.N	Models	Vult Push. (kN)	Vult Cycli (kN)	Difference (kN)	Difference Percentage %
1	B31	250	241.0	9.0	0.04
2	B32	250	230.0	20.0	0.08
3	B33	257	241.0	16.0	0.06
4	B34	273	234.0	39.0	0.14
5	C31	220	215.0	5.0	0.02
6	C32	212	203.0	9.0	0.04
7	C33	225	221.0	4.0	0.02
8	C34	231	215.0	16.0	0.07

**Table (11) Comparing displacement results for model B3i and C3i (i=1, ..., 4)**

S.N	Models	$\Delta$ ult Push. (kN)	$\Delta$ ult Cycli (kN)	Difference (kN)	Difference Percentage %
1	B31	26.0	26.0	0.0	0.00
2	B32	20.0	26.0	-6.0	-0.30
3	B33	22.4	26.0	-3.6	-0.16
4	B34	25.2	28.0	-2.8	-0.11
5	C31	25.0	29.0	-4.0	-0.16
6	C32	15.0	21.0	-6.0	-0.40
7	C33	18.0	27.0	-9.0	-0.50
8	C34	26.6	26.0	0.6.0	0.020

From these tables one can conclude that;

(i) The best result for ultimate displacement with the minimum variation occurs for models B2i and C2i, with 4% (in average) difference for ductility (maximum 12%) which is good enough to accept the results. The largest differences belong to models B32, C32 and C33. The error for these models can be justified by post yielding analysis error. For other models these differences vary between 0 and 23% with an average of 12.8% that could be acceptable.

(ii) Ultimate strengths which are the peak points of load–displacement curves are summarized in Tables 4 and 5 for all models and both cyclic and pushover loads. As it can be seen, there is no significant changes in magnitudes of ultimate strengths due to any changes in joint dimensions or joint reinforcement for both cyclic and pushover loadings. This can be explained by the failure mode of the joint and modeling characteristics. For example, if failure mode is a flexural type, then joint core reinforcement might not participate in joint strength, besides it is also possible that the model is not capable to simulate the confinement of the joint core reinforcement, completely. This phenomenon needs more investigation. The best achieved strength among all models belongs to models B2i and C2i which have the same cross sections for both beams and columns.

(iii) The computed displacement ductilities,  $\mu$ , are provided in the sixth column of Tables 3 and 4. The best achieved ductility for each series of models belongs to Bi4 and Ci4 models ( $i=1, 2, 3$ ). Models Bi1, Ci1 ( $i=1, 2, 3$ ) show good ductilities. Models Bi2, Ci2 and Bi3, Ci3 have a ductility problem. In general, if computed ductility of a model is between 1.2 to 3.11 it is not good enough.

(iv) Variations in ultimate strength and displacement with respect to the change in joint reinforcement for some models can be seen in Fig. 8. For almost all models with the same beam and column sizes, both ultimate strength (peak of the curve) and ultimate displacement (the point of 15% decrease in strength) move up by increasing the joint core reinforcement ( $\rho_s$ ) and these models demonstrate better behavior.

Although the increase of ultimate strength is not significant, there is considerable variation in ultimate displacement. The area under the curve is proportionally varying by the amount of joint reinforcement. In general, it can be concluded that, an increase in joint reinforcement will improve joint performance (ultimate strength, displacement ductility and energy dissipation).

#### 4. CONCLUSION

The aim of this research is to develop a F.E. model for RC beam column connections in the simulation environment provided by ANSYS, in order to study the behavior of RC beam-column joints subjected to seismic forces using the developed model. A detailed process of developing and verifying a robust F.E. model for a RC beam column connection is presented. After modeling many joints and post processing the results, the conclusions are summarized as follows:

##### a) Simulation Characteristics:

- 1- ANSYS can be used for both modeling and detecting damage in an existing RC structure. But in order to be able to observe a specific behavior from the model, the required modeling parameters must be defined and adjusted properly.
- 2- Both cyclic dynamic and pushover results of the considered F.E. models show acceptable matching with the real test data.
- 3- Pushover static test presents up to 15% increase in strength compared to cyclic dynamic test.

##### b) Effect of joint transverse steel ratio:

- 1-The joint joint transverse steel ratio ( $\rho_s$ ) improves joint seismic performance.
- 2- The joint transverse steel ratio significantly affects the displacement ductility and post failure behavior of a connection.
- 3- Increasing joint transverse steel ratio does not significantly affect joint ultimate strength.

##### c) Moment Capacity Ratios and Shear Capacity Ratios:

- 1- Models with greater (significantly more than 1.0) shear capacity ratios, VR, and moment capacity ratios, MR, have the capabilities to resist forces with magnitudes 70% up to 100% more than code requirements.
- 2- Beams in models with moment capacity ratios, MR, significantly greater than 1.0, resist forces more than their expected capacities assigned by the design code.
- 3- For models with moment capacity ratios less than 1.2 (which is code requirement), and shear capacity ratios less than 1.0, the O.S.F. decreases and failure occurs at O.S.F about 1.0.
- 4- For models with moment capacity ratios greater than 1.2 and shear capacity ratio more than 1.0, ultimate strength is 40% to 50% more than code requirements, which makes them safe.

##### Recommendations:

1. The current investigation can be extended to reinforced concrete exterior beam-column joints to study the seismic behavior and post-peak performance of exterior joints with various parameters under reversed cyclic loading and earthquake excitation.

2. The influence of transverse beams and floor slabs can be studied to identify their contributions to resisting seismic loading under in-plane and out-of-plane loads.

3. Several wide beam specimens were simulated in this research to reveal the stress transfer paths in wide beam-column joints. More specimens should be considered to improve the understanding of load paths of wide beam-column connections with various geometries and design parameters, such as beam width and depth, column height, beam-to-column eccentricity, etc.

## 5. REFERENCES

- [1] The Egyptian design codes.
- [2] JianBing Yu et al (2020), Seismic behavior of precast concrete beam-column joints with steel strand inserts under cyclic loading, *Engineering Structures* 216 (2020) 110766.
- [3] ACI-ASCE Committee352. (2002). Recommendations for design of beam-column joints in monolithic reinforced concrete structures. ACI 352R-02, American Concrete Institute, Detroit, U.S.A.
- [4] Xinyu Shen et al (2021), Seismic performance of reinforced concrete interior beam-column joints with novel reinforcement detail, *Engineering Structures* 227 (2021) 111408.
- [5] Rajai Z. Al-Rousan (2022), Cyclic behavior of alkali-silica reaction-damaged reinforced concrete beam-column joints strengthened with FRP composites, *Case Studies in Construction Materials* 16 (2022) e00869.
- [6] Hanson, N. W. (1971). Seismic resistance of concrete frames with Grade 60 reinforcement. *Proceedings, ASCE*, Vol. 97(ST6), pp. 1685-1700.
- [7] ACI-ASCE Committee352. (1976). Recommendations for design of beam-column joints in monolithic reinforced concrete structures. ACI 352R-76, American Concrete Institute, Detroit, U.S.A.
- [8] Murty, C. V. R., Rai, D. C., Bajpai, K. K. & Jain, S. K. (2003). Effectiveness of reinforcement details in exterior reinforced concrete beam-column joints for earthquake resistance. *ACI Structural Journal*, Vol. 100, No. 2, pp.149-156.
- [9] Megget, L. M. (1974). Cyclic behavior of exterior reinforced concrete beam-column joints. *Bulletin of the New Zealand National Society for Earthquake Engineering*, Vol. 7, No. 1, pp. 27-47.
- [10] Paulay T., Park, R. & Priestley, M. J. N. (1978). Reinforced concrete beam-column joints under seismic actions. *ACI Structural Journal*, Vol. 75, No. 11, pp. 585-593.
- [11] Paulay, T. & Scarpas, A. (1981). The behavior of exterior beam-column joints. *Bulletin of the New Zealand National Society for Earthquake Engineering*, Vol. 14, No. 3, pp. 131-144.
- [12] Durrani, A. J. & Wight, J. K. (1985). Behavior of interior beam-to-column connections under earthquake type loading. *ACI Structural Journal*, Vol. 82, No. 3, pp. 343-349.
- [13] Ehsani, M. R. & Wight, J. F. (1985). Exterior reinforced concrete beam-to-column connections subjected to earthquake-type loading. *ACI Structural Journal*, Vol. 82, pp. 492-499.
- [14] Kitayama, K., Otani, S. & Aoyama, H. (1987). Earthquake resistant design criteria for reinforced concrete interior beam-column joints. *Proceedings of Pacific Conference on Earthquake Engineering*. Wairakei, New Zealand, August 5-8, Vol. 1, pp. 315-326.
- [15] Tsonos, A. G, Tegos, I. A. & Penelis, G. (1992). Seismic resistance of type 2 exterior beam-column joints reinforced with inclined bars. *AIC Structural Journal*, Vol. 89, pp. 3-12.
- [16] Agbabian, M, Higazy, E. M. & Abdel-Ghaffar, A. M. (1994). Experimental observations on the seismic shear performance of RC beam-to-column connections subjected to varying axial column force. *Earthquake Engineering and Structural Dynamics*, Vol. 23, pp. 859-876.
- [17] Hakuto, S, Park, R. & Tanaka, H. (2000). Seismic load tests on interior and exterior beam-column joints with substandard reinforcing details. *ACI Structural Journal*, Vol. 97, No. 1, pp. 11-25.
- [18] Hwang, S. J., Lee, H. J. & Wang, K. C. (2004). Seismic design and detailing of exterior reinforced concrete beam-column joints. *13th World Conference on Earthquake Engineering*. Vancouver, Canada, August 1-8, Paper No. 397.
- [19] Hwang, S. J., Lee, H. J., Liao, T. F., Wang, K. C. & Tsai, H. H. (2005). Role of hoops on shear strength of reinforced concrete beam-column joints. *ACI Structural Journal*, Vol. 102, No. 3, pp. 445-453.
- [20] Tsonos, A. G. (2007). Cyclic load behavior of reinforced concrete beam-column sub-assemblages of modern structures. *ACI Structural Journal*, Vol. 104, 4), pp.468-478.
- [21] Bindhu, K. R., Sukumar, P. M. & Jaya, K. P. (2009). Performance of exterior beam-column joints under seismic type loading. *ISET Journal of Earthquake Technology*, Vol. 46, No. 2, pp. 47-64.

- 
- [22] Bindhu, K. R. & Sreekumar, K. J. (2011). Seismic resistance of exterior beam-column joint with diagonal collar stirrups. *International Journal of Civil and Structural Engineering*, Vol. 2, No. 1, pp. 160-175.
- [23] Asha, P. & Sundararajan, R. (2012). Seismic behavior of exterior beam-column joints with square spiral confinement. *Asian Journal of Civil Engineering (Building and Housing)*, Vol. 13, No. 4, pp. 571-583.
- [24] Mostofinejad, D. & Talaeitaba, S. B. (2006). Finite element modeling of RC connections strengthened with FRP laminates. *Iranian Journal of Science and Technology, Transaction B*, Vol. 30, No. B1, pp. 21-30.
- [25] Dalalbashi Esfahani, A., Mostofinejad, D., Mahini, S. & Ronagh, H. R. (2011). Numerical investigation on the behavior of FRP retrofitted RC exterior beam-column joints under cyclic loads. *Iranian Journal of Science and Technology, Transactions of Civil and Environmental Engineering*, Vol. 35, No. C1, pp. 35-50.
- [26] Arslan, M. H. & Gulay, F. G. (2009). Numerical study on seismic behavior of precast concrete connection zone. *Iranian Journal of Science and Technology, Transaction B*, Vol. 33, No. B1, pp. 123-127.
- [27] ANSYS, Inc., (2021), "ANSYS Help", Release 11.0, Documentation copyright.